Oxytocin/vasopressin-like peptide inotocin regulates cuticular hydrocarbon synthesis and water balancing in ants

Akiko Koto[a,b,1], Naoto Motoyama[c], Hiroki Tahara[c], Sean McGregor[d], Minoru Moriyama[a,b], Takayoshi Okabe[e], Masayuki Miura[c], and Laurent Keller[d]

[a]Bioproduction Research Institute, National Institute of Advanced Industrial Science and Technology, Tsukuba, 305-8566 Ibaraki, Japan; [b]Computational Bio Big Data Open Innovation Laboratory (CBBD-OIL), National Institute of Advanced Industrial Science and Technology, Tsukuba, 305-8566 Ibaraki, Japan; [c]Department of Genetics, Graduate School of Pharmaceutical Sciences, The University of Tokyo, 113-0033 Tokyo, Japan; [d]Department of Ecology and Evolution, University of Lausanne, CH-1015 Lausanne, Switzerland; and [e]Drug Discovery Initiative, The University of Tokyo, 113-0033 Tokyo, Japan

Edited by Bert Hölldobler, Arizona State University, Tempe, AZ, and approved February 1, 2019 (received for review October 17, 2018)

Oxytocin/vasopressin-like peptides are important regulators of physiology and social behavior in vertebrates. However, the function of inotocin, the homologous peptide in arthropods, remains largely unknown. Here, we show that the level of expression of inotocin and inotocin receptor are correlated with task allocation in the ant *Camponotus fellah*. Both genes are up-regulated when workers age and switch tasks from nursing to foraging. in situ hybridization revealed that *inotocin receptor* is specifically expressed in oenocytes, which are specialized cells synthesizing cuticular hydrocarbons which function as desiccation barriers in insects and for social recognition in ants. dsRNA injection targeting *inotocin receptor*, together with pharmacological treatments using three identified antagonists blocking inotocin signaling, revealed that inotocin signaling regulates the expression of *cytochrome P450 4G1* (*CYP4G1*) and the synthesis of cuticular hydrocarbons, which play an important role in desiccation resistance once workers initiate foraging.

social insect | oxytocin/vasopressin-like peptide | division of labor | behavioral tracking | cuticular hydrocarbon

In humans and mammals, the neuropeptide hormones oxytocin and vasopressin are involved in a number of physiological processes and are increasingly implicated in a variety of social behaviors. In particular, oxytocin signaling regulates uterine contraction, lactation, and energy metabolism and has been demonstrated to increase levels of parental care, pair bonding, and cooperation (1–4). Vasopressin is important for water balancing via the control of antidiuresis and regulation of blood pressure and plays a role in influencing social behaviors such as territorial defense, aggression, and also pair bonding (5–8). Across vertebrates, oxytocin/vasopressin-like peptide homologs appear to have conserved physiological (9, 10) and behavioral functions (11–15).

An increasing number of genomic and transcriptomic analyses have revealed that a further homolog, inotocin, is specific to invertebrates, where it is conserved across at least 100 species (16). This places the origin of the oxytocin/vasopressin-like peptide family before the split of the Protostomia and Deuterostomia, >600 Mya (17). Studies on inotocin signaling in insects (16, 18–22) suggest a possible role in diuresis in *Tribolium castaneum* (18) and locomotor activity in ants (21). However, the molecular and cellular functions of inotocin signaling remain largely unknown. Given the important role of oxytocin/vasopressin-like peptides in regulating social behavior in vertebrates (23–25), we conducted a study using ants as a model organism to investigate the physiological role of inotocin signaling and its potential implication in social behavior.

Ants live in large and complex societies consisting of one or more reproductive queens and many nonreproductive workers (26). Workers exhibit division of labor with individuals performing specific tasks within a colony (27–29). Individual task preference is generally correlated with age, with younger workers remaining inside the nest to nurse the developing offspring and older workers foraging outside the nest. This age-based division of labor is often referred to as task polyethism, although individuals may also flexibly switch their role according to colony demands (30–32).

As workers transit from nursing to foraging, they experience new environmental challenges, such as fluctuating temperatures and low humidity, both significant threats in terms of water loss and desiccation. Previous work on various insects showed that cuticular hydrocarbons (CHCs) on the body surface play an important role in protecting against desiccation (33–35). CHCs also play an important role in social recognition (36), especially to distinguish nestmates from nonnestmates in ants (37–39). It has been reported that workers change their CHC profiles before initiating foraging (40–43), possibly to better cope with the drier environment that they will encounter outside of the nest. However, the mechanisms regulating these changes remain largely unknown.

In this study, we first compare the expression of inotocin signaling in different castes and body parts of two ant species of the genus *Camponotus* and then use genetic and pharmacological manipulations to investigate the possible physiological function of this pathway. We found that inotocin and its receptor are most highly expressed in workers, particularly foragers, whereas queens and males show low expression levels. Histological analyses revealed that *inotocin receptor* is specifically expressed in the oenocytes, a type of specialized cell that produces CHCs in insects (44–46). We also show that inotocin signaling regulates the expression of CHCs

Significance

Inotocin, the oxytocin/vasopressin-like peptide, is widely conserved in arthropods; however, little is known about its molecular function. Here, we show that, in ants, the expression levels of *inotocin* and its receptor are correlated with the age of workers and their behavior. We also demonstrate that inotocin signaling is involved in desiccation resistance by regulating the synthesis of cuticular hydrocarbons. We propose that the up-regulation of *inotocin* and its receptor as workers age and switch tasks from nursing to foraging is a key physiological adaption to survive drier environments outside of the nest.

Author contributions: A.K. and M. Miura designed research; A.K., N.M., H.T., S.M., M. Moriyama, and T.O. performed research; A.K. contributed new reagents/analytic tools; A.K., N.M., H.T., S.M., T.O., M. Miura, and L.K. analyzed data; and A.K. and L.K. wrote the paper.

The authors declare no conflict of interest.

This article is a PNAS Direct Submission.

[1]To whom correspondence should be addressed. Email: a-koto@aist.go.jp.

This article contains supporting information online at www.pnas.org/lookup/suppl/doi:10.1073/pnas.1817788116/-/DCSupplemental.

Published online March 6, 2019.

via *CYP4G1*, the key enzyme for hydrocarbon synthesis (45, 46). Based on these results, we propose that inotocin signaling is a key regulator of hydrocarbon metabolism, which in turn may allow an adaptive plastic response as workers transition from the relatively safe environment of the nest to a hostile foraging environment.

Results

Expression Profiles of int/intR in Reproductive Castes. To compare the expression levels of *inotocin* (*int*) and *inotocin receptor* (*intR*) among castes, we collected young virgin queens, mated queens, males, and workers of the carpenter ant *Camponotus japonicus* in 2016. There was substantial variation in levels of *int* mRNA among body parts (head, thorax, and abdomen; $F_{49} = 47.3$, $P < 0.0001$) and castes (virgin queens, mated queens, males, and workers; $F_{49} = 30.2$, $P < 0.0001$), as well as a significant interaction between body parts and castes ($F_{49} = 31.4$, $P < 0.0001$; Fig. 1*A* and *SI Appendix*, Table S1). In the head, the level of expression was high in workers, intermediate in the two types of queens, and low in males. In the thorax, the levels of expression were very low in each of the four castes, while in the abdomen, the levels of expression were intermediate, with no significant differences among castes.

The expression of *intR* was significantly different between body parts ($F_{53} = 11$, $P = 0.0001$) and castes ($F_{53} = 18.3$, $P < 0.0001$). There was also a significant interaction between body parts and castes ($F_{53} = 12.2$, $P < 0.0001$; Fig. 1*B* and *SI Appendix*, Table S1). In the head and thorax, *intR* expression was very high in workers, intermediate in queens, and very low in males. In the abdomen, the level of expression was significantly higher in workers than males and the two types of queens. Similar results were obtained in *C. japonicus* samples collected in 2015 (Fig. 1 *C* and *D* and *SI Appendix*, Table S1).

To investigate the role of inotocin signaling on social behavior, we conducted a detailed analysis of the expression of *int* and *intR* in workers. Because it is difficult to control for worker age and precisely determine worker task in the field, we used *Camponotus fellah* workers from colonies established from founding queens collected in 2003 and 2007 throughout all of the following experiments. We first confirmed that the expression profiles in reproductive castes of *C. fellah* are similar with those of *C. japonicus* (*SI Appendix*, Fig. S1 and Table S1), with the difference that the expression of *int* mRNA is higher in the heads of males than queens and workers.

Correlation Between *int/intR* Expression and Task Allocation in Workers. To determine the approximate age of each worker in the laboratory-reared *C. fellah* colonies, we color-marked newly eclosed workers every month. Task allocation was defined by the spatial location of the ants in the rearing box, with "nurses" being workers collected in the nest and "foragers" those in the foraging arena (Fig. 2*A*). There was a significant association between age and foraging propensity ($\chi^2 = 255.2$, $P < 0.0001$; Fig. 2*B*). Individuals started foraging after they were 4 mo old with a significant increase in the proportion of foraging with increased age (Fig. 2*B* and *SI Appendix*, Fig. S2 *A*–*C*).

Given that *int* is predominantly expressed in the heads (Fig. 1 *A* and *C* and *SI Appendix*, Fig. S1*A*), we compared the expression profiles of *int* in the heads of nurses and foragers of different age classes. *int* expression was significantly associated with age ($F_{184} = 3.6$, $P = 0.0023$) and task ($F_{186} = 4.4$, $P = 0.037$; age × task interaction: $F_{185} = 0.056$, $P = 0.94$). The level of expression of *int* was lowest in young nurses and highest in old foragers (Fig. 2*C*). The level of *int* expression was also significantly higher in foragers than nurses within one of the three age classes containing both types of workers (5-mo-old individuals: $F_{30} = 4.8$, $P = 0.037$; *SI Appendix*, Table S2). Given that *intR* is predominantly expressed in the abdomen (Fig. 1 *B* and *D* and *SI Appendix*, Fig. S1*B*), we compared the expression profiles of *intR* in the abdomens of nurses and foragers of different age classes. Similar to *int* in the head, there was a significant effect of age on *intR* expression ($F_{178} = 26.5$, $P < 0.0001$; Fig. 2*D*) and an interaction effect between age and task ($F_{178} = 4.2$, $P = 0.017$), but *intR* expression was not significantly associated with task ($F_{178} = 0.37$, $P = 0.54$). There was, however, a significant difference in *intR* expression between nurses and foragers within two of the three age classes containing both types of workers (5-mo-old individuals: $F_{34} = 10.8$, $P = 0.0024$; 6-mo-old individuals: $F_{31} = 5.3$, $P = 0.028$; *SI Appendix*, Table S2). These results suggest that *int* and *intR* expression are associated not only with age, but also with the task performed by workers.

To further investigate the role of *int* and *intR* on division of labor and to control for age-dependent effects, we set up nine groups, each containing 10 4-mo-old nurses, and monitored their behavior as division of labor was reorganized with those that remained as nurses and others who started foraging. We measured activity level, time in the food region, and time in the nest (Fig. 2*E* and *SI Appendix*, Fig. S2*D*) with an automated video-tracking system (47) during 6 d. The level of *int* expression in the whole body was positively correlated with the overall level of activity ($F_{71} = 48.9$, $P < 0.0001$; Fig. 2*G*), but not the amount of time spent in the food region ($F_{71} = 2.3$, $P = 0.13$; Fig. 2*F*) or time spent in the nest ($F_{71} = 0.25$, $P = 0.62$; Fig. 2*H*). The level of expression of *intR* was not significantly correlated with any of these three behavioral measures (time in the food region: $F_{70} = 0.14$, $P = 0.71$, Fig. 2*I*; distance covered: $F_{70} = 1.24$, $P = 0.27$, Fig. 2*J*; time in

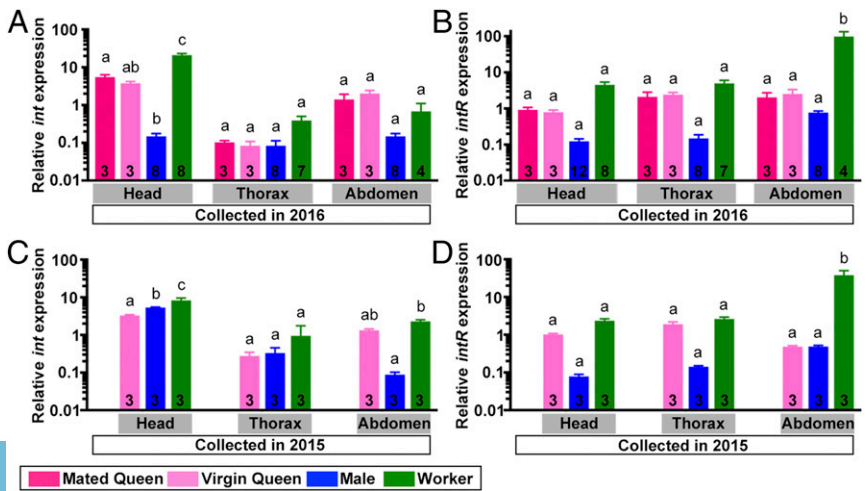

Fig. 1. Relative expression of *int* and *intR* in different castes and tissues of *C. japonicus*. Relative expression (mean ± SEM) of *int* (*A* and *C*) and *intR* (*B* and *D*) in the head, thorax, and abdomen of mated queens (red), virgin queens (pink), males (blue), and workers (green) is shown. The expression of each gene was scaled by the average value in each graph. Values are therefore not comparable between graphs. Number of individuals are shown in each box. The relative expression levels of each gene were tested with two-way ANOVA. Groups differing significantly ($P < 0.05$) are marked with different letters. Samples shown in *A* and *B* were collected in 2016 and samples in *C* and *D* in 2015. We did not collect any mated queens in 2015.

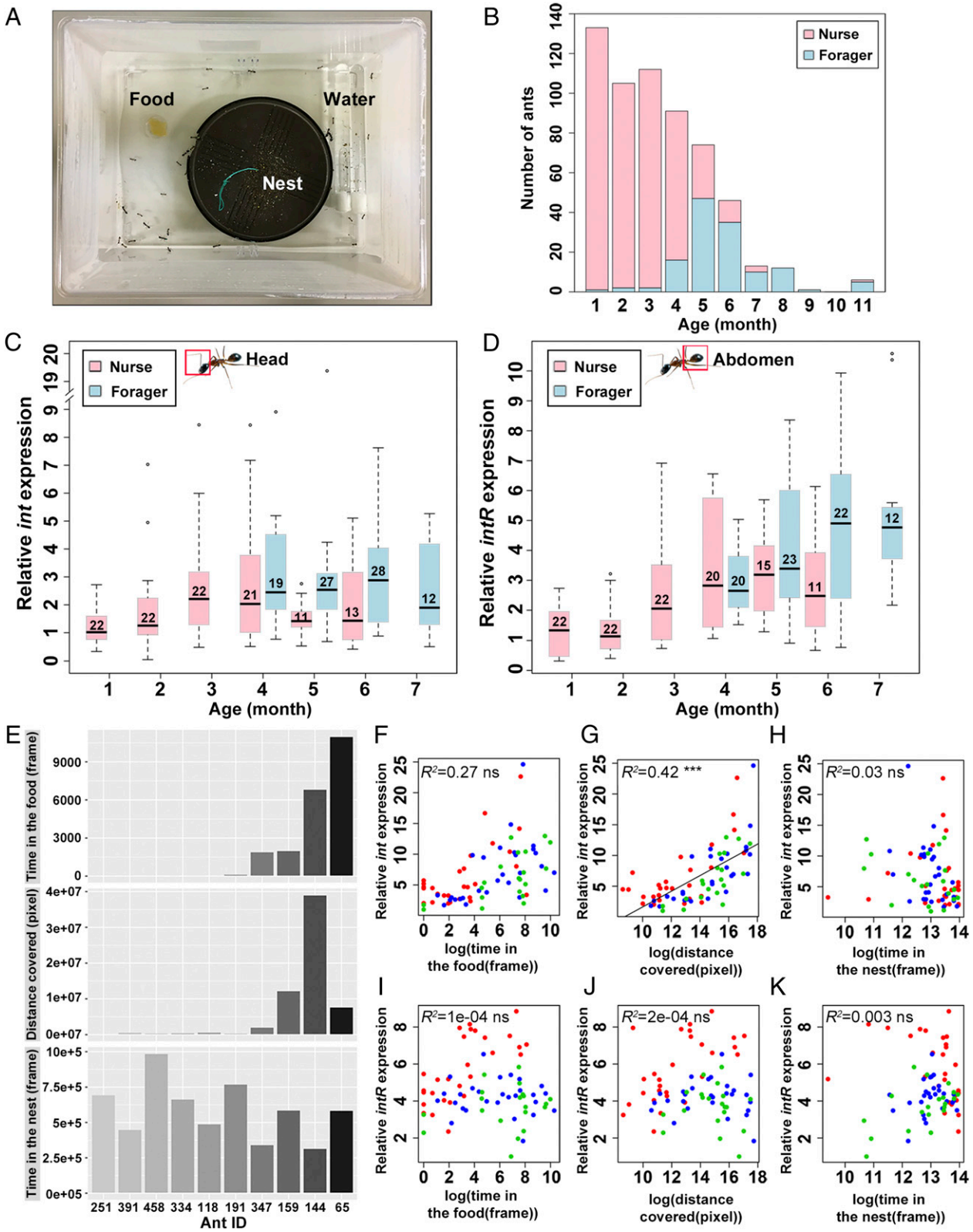

Fig. 2. Correlation between the expression of inotocin signaling and task allocation. (*A*) Setup of the *C. fellah* colonies. (*B*) Age-dependent division of labor in one representative colony. Nurses are shown in pink and foragers in light blue. (*C* and *D*) Box plots of the relative expression levels of *int* in the head (*C*) and *intR* in the abdomen (*D*) for each age class. Number of individuals is shown in each box. (*E*) The time spent in the food region and in the nest and distance moved was quantified over 6 d in the tracking system for one representative box. (*F–H*) Relationship between the behavioral parameters and *int* expression. (*I–K*) Relationship between the behavioral parameters and *intR* expression. Different colors indicate the colony of origin of workers. R^2 and *P* values are shown in the top left of the graphs. The correlation between the expression of *int* or *intR* and behavioral parameters were tested with a generalized linear mixed model (GLMM). ns, $P > 0.05$; ***$P < 0.001$.

the nest: $F_{70} = 3.79$, $P = 0.06$, Fig. 2*K*). A similar experiment conducted with younger (1- to 2-mo-old) workers (*SI Appendix*, Fig. S3) revealed a similar pattern for *int,* but the level of expression of *intR* was also significantly associated with the overall level of activity (*int*: $F_{43} = 12.3$, $P = 0.001$, *SI Appendix*, Fig. S3*F*; *intR*: $F_{44} = 21.2$, $P < 0.0001$, *SI Appendix*, Fig. S3*I*). These results further support the view that the expression levels of *int* and *intR* are both associated with the age and the behavior of workers.

Cellular Localization of *int* and *intR* in Workers. To better understand the function of inotocin signaling, we next looked for cellular localization of *int* in the head and *intR* in the abdomen of workers. Fluorescence in situ hybridization with an *int* gene probe revealed highly specific expression of *int* mRNA in one pair of neurons of the subesophageal zone (indicated with arrowheads in Fig. 3*A* and magnified in Fig. 3 *B* and *C*). This expression pattern is similar to that of anti-vasopressin antibody staining in locusts (18) and the ant *Lasius neglectus* (21). To further clarify the localization of inotocin proprotein, we created an antibody against the inotocin proprotein (anti-int) targeting the C terminus region of the inotocin proprotein (*SI Appendix*, Fig. S4 *A*–*C*). To examine whether the expression of *int* mRNA and its proprotein were in the same cells of the subesophageal zone, we performed sequential staining with immunohistochemistry and fluorescence in situ hybridization, which confirmed that the two neurons of the subesophageal zone expressing *int* mRNA were also labeled with anti-int antibody (shown in *SI Appendix*, Fig. S4 *D*, *Upper*). By contrast, no signal was found when performing a negative-control immunostaining with an anti-int antibody preabsorbed with the antigen peptide (*SI Appendix*, Fig. S4 *D*, *Lower*), consistent with specificity of the immunoreactive signals labeled with anti-int antibody.

In addition to a pair of neurons in subesophageal zone (indicated with arrowheads in Fig. 3*D*), we identified a cluster of neurons labeled with anti-int antibody in the protocerebrum (Fig. 3*E*). They spread from the subesophageal zone to the lateralis of the medial superior protocerebrum (indicated with arrows in Fig. 3 *D* and *E*). Cytoplasmic immunoreactivity of anti-int antibody on the lateralis of protocerebrum (indicated with arrowheads in Fig. 3*E*) was very similar to the neurosecretory neurons expressing PERIOD in

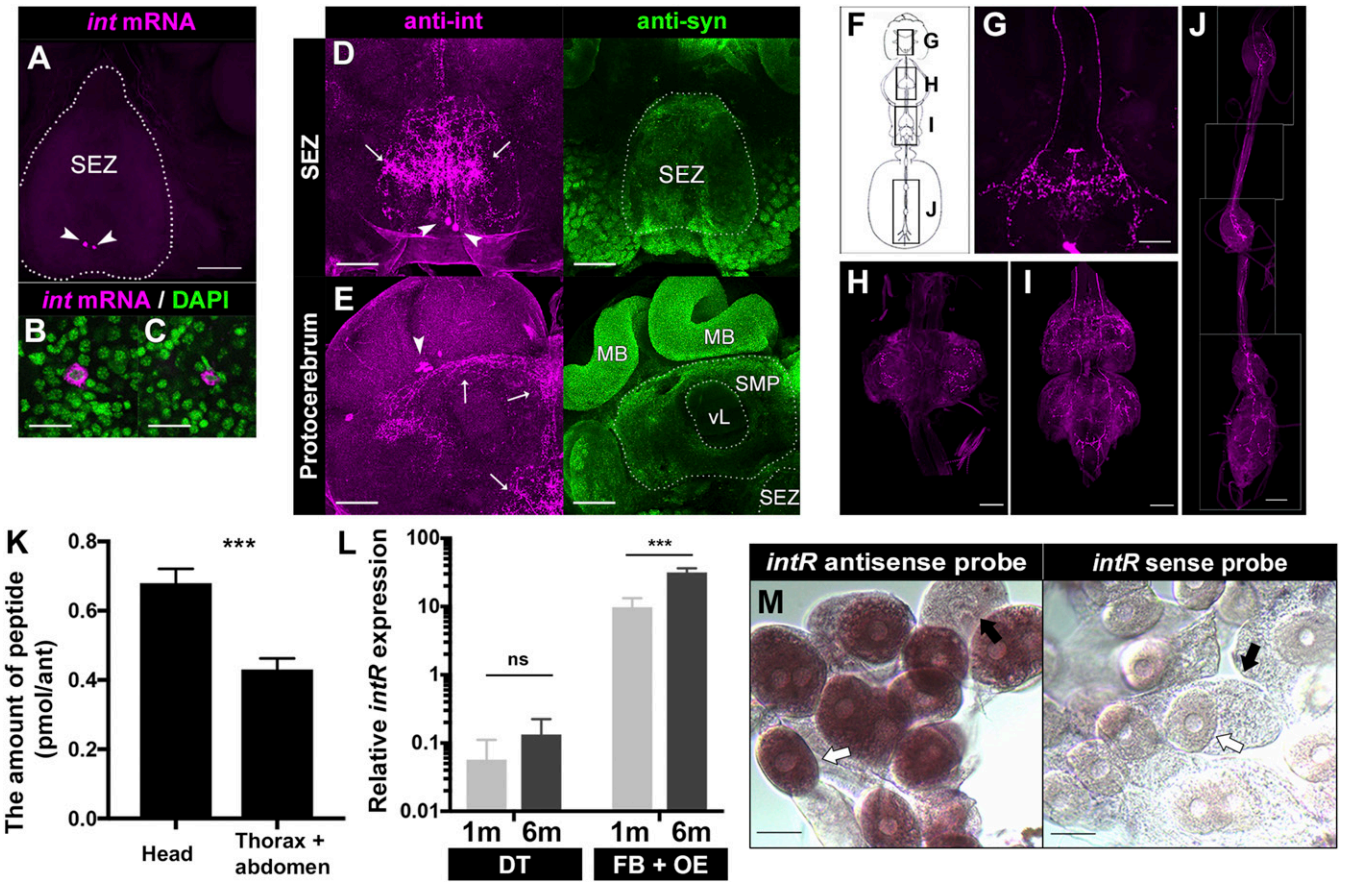

Fig. 3. The expression of *int* in neural tissues and *intR* in the fat body plus oenocytes. (*A*) Fluorescence in situ hybridization using a specific *int* antisense probe (shown in magenta). Arrowheads indicate the pair of neurons labeled with *int* mRNA in the subesophageal zone (SEZ, outlined with white dotted line). (*B* and *C*) Magnified image of each *int* mRNA-positive neuron (shown in magenta in *A*) with stained nucleus using DAPI (shown in green). (*D* and *E*) Immunohistochemistry for anti-int antibody (shown in magenta) and anti-synapsin antibody (shown in green) in SEZ (*D*) and protocerebrum (*E*). Arrowheads indicate cytoplasmic expression of anti-int immunoreactivity. Arrows indicate the neurons positive with anti-int antibody in SEZ (*D*) and protocerebrum (*E*), in which brain compartments are labeled as mushroom body (MB), medial superior protocerebrum (SMP), and vertical lobe (vL). (*F*) Schematic presentation from central to peripheral nervous system in workers. (*G*–*J*) One pair of neurons labeled with anti-int antibody from the subesophageal zone to the ventral nerve cord (*G*), the prothoracic (*H*), mesothoracic and metathoracic (*I*), and abdominal ganglia (*J*). (*K*) Distribution of endogenous inotocin peptide tested with unpaired two-tailed *t* test. ***$P < 0.001$. (*L*) qRT-PCR for the *intR* in the digestive tract (DT) and fat body plus oenocytes (FB+OE). The expression of *intR* mRNA was tested with GLMM with Benjamini–Hochberg post hoc test. ns, $P > 0.05$; ***$P < 0.001$. (*M*) in situ hybridization using an *intR* antisense probe (*Left*) and sense probe (*Right*) in the dissected fat body plus oenocytes. Oenocytes are indicated with open arrows and trophocytes (the lipid-storing cells of the fat body) with filled arrows. [Scale bars, 100 μm (*A*, *D*, *E*, and *G*–*J*) and 20 μm (*B*, *C*, and *M*).]

honey bees (48), suggesting that these immunoreactive neurons may also have a neurosecretory role.

Additional immunohistochemistry with anti-int antibody revealed a pair of descending axons coming from the cell bodies in the subesophageal zone, which are spanning the length of the ventral nerve cord (Fig. 3 *F* and *G*) and extending through the prothoracic (Fig. 3*H*), mesothoracic, metathoracic (Fig. 3*I*), and abdominal ganglia (Fig. 3*J*).

We next examined the expression profile of endogenous inotocin peptide between the head, thorax, and abdomen of 6-mo old foragers. Liquid-chromatography–tandem MS (LC-MS/MS) revealed the distribution of inotocin peptide between tissues, with the highest level of inotocin peptide in the head ($t_{10} = 4.8$, $P = 0.0007$; Fig. 3*K*). This result is consistent with the highest expression of *int* mRNA in the head, suggesting that the inotocin peptide is mainly expressed in the central nervous system, as is the case with oxytocin and vasopressin in mammals. In addition, the distribution of inotocin peptide in the thorax and abdomen suggests that inotocin peptide could activate its receptor, which is highly expressed in the abdomen (Figs. 1 *B* and *D* and 2*D*).

Next, we examined in which specific tissues of the abdomen *intR* was expressed. We focused on the digestive tract, fat body, and oenocytes, which are interspersed within the fat body in ants (49, 50). Because it is technically very difficult to separate oenocytes from the fat body, we extracted RNA from the fat body plus oenocytes. We found that *intR* mRNA was expressed at significantly greater levels in the fat body plus oenocytes than in the digestive tract (age effect, $F_{30} = 148$, $P < 0.0001$; tissue effect, $F_{30} = 525$, $P < 0.0001$; tissue × age interaction, $F_{30} = 145$, $P < 0.0001$; Fig. 3*L*), implicating the fat body or oenocytes as a likely tissue expressing *intR* in the abdomen. In addition, there was a strong age effect ($P < 0.0001$; Fig. 3*L*) with 6-mo-old workers expressing significantly higher levels of *intR* in the fat body plus oenocytes than 1-mo-old workers. This result is consistent with expression data from the whole abdomen (Fig. 2*D*).

To determine the source of *intR* expression at the cellular level, we conducted in situ hybridization. These analyses revealed specific expression in the oenocytes, which can be recognized by their round-shaped nucleus (open arrows, Fig. 3 *M*, *Left*). By contrast, there was no signal in the trophocytes, which are the main cells of the fat body and are recognizable by their irregular nucleus (filled arrows, Fig. 3 *M*, *Left*). Together, these data indicate that the inotocin proprotein is expressed in the central and peripheral nervous systems and then transferred through to the abdomen, where it likely activates inotocin receptor sites specifically expressed in the oenocytes.

Correlation Between *intR* and *CYP4G1* Expression. Given that *intR* is expressed in oenocytes, we investigated the relationship between inotocin signaling and the CHC synthesis pathway to which the cells' primary function is linked. We first focused on the *CYP4G1* gene, which is an aldehyde oxidative decarbonylase P450. This gene is highly conserved in insects and is known to be expressed in the oenocytes (44–46), where it regulates the final step of CHC synthesis by converting aldehyde to hydrocarbons (45). We found higher expression of *CYP4G1* in the fat body plus oenocytes than in the digestive tract (age effect, $F_{30} = 12.4$, $P = 0.0014$; tissue effect, $F_{30} = 220$, $P < 0.0001$; tissue × age interaction, $F_{30} = 9.8$, $P = 0.0038$; Fig. 4*A*). The expression of *CYP4G1* was higher in the fat body plus oenocytes of 6-mo than 1-mo-old workers ($P < 0.0001$; Fig. 4*A*). A similar pattern was found by using a specific antibody against CYP4G1 protein, with CYP4G1 expressed in the fat body plus oenocytes, but not in the digestive tract (Fig. 4*B*). Immunohistochemistry with this antibody further revealed that the CYP4G1 protein is specifically expressed in the oenocytes, but not in the trophocytes (Fig. 4*C*). In addition to the similarity between the histological expression of CYP4G1 (Fig. 4*C*) and *intR* (Fig. 3*M*), the expression of *CYP4G1* mRNA is up-regulated in an age-dependent manner both in the head (*SI Appendix*, Fig. S5*A*) and abdomen (*SI Appendix*, Fig. S5*B*), and there was also a positive correlation between the expression of these two genes in the abdomen ($R^2 = 0.58$, $t_{32} = 6.6$, $P < 0.0001$; Fig. 4*D*).

To study the relationship between inotocin signaling and *CYP4G1* expression, we performed an RNA interference assay by feeding 5-mo-old workers with dsRNA targeting *intR* with the described protocol (51). Workers fed with dsRNA of *intR* showed a lower level of expression of *intR* in the abdomen than control ants ($t_{16} = 3.3$, $P = 0.0044$; Fig. 4*E*). Moreover, the expression of the *intR* was significantly correlated with the expression of *CYP4G1* in both ants treated with dsRNA of *intR* ($R^2 = 0.76$ $t_8 = 5.04$, $P = 0.001$; Fig. 4*F*) and control ants treated with dsRNA of *GFP* ($R^2 = 0.97$, $t_6 = 14.36$, $P < 0.0001$; Fig. 4*F*), resulting in the down-regulation of *CYP4G1* expression in the dsRNA of *intR*-treated ants ($t_{16} = 4.06$, $P = 0.0009$; Fig. 4*G*).

Identification of Antagonists That Block Inotocin Signaling. We next developed a pharmacological protocol to inhibit inotocin signaling. We established a Chinese hamster ovarian (CHO) cell line which stably expressed the inotocin receptor and monitored the activation of the receptor against inotocin peptide by measuring the increase in cytosolic calcium concentration with the fluorescent calcium probe Fluo-4. We confirmed that the inotocin receptor is activated by the synthesized inotocin peptide in a dose-dependent manner ($EC_{50} = 1.09$ nM; Fig. 5*A*) as described (21, 22, 52). We also showed that the inotocin receptor is activated by oxytocin ($EC_{50} = 41.6$ μM; Fig. 5*A*), but not vasopressin (Fig. 5*A*), suggesting the possibility that oxytocin antagonists may also inhibit inotocin signaling. To test this, we used atosiban, an oxytocin analog with the modification of amino acids at 1, 2, 4, and 8, which is medically used for the treatment of preterm labor (53). The activation of the inotocin receptor by inotocin was inhibited by atosiban in a dose-dependent manner ($IC_{50} = 599$ μM; Fig. 5*B*), although this effect was weaker than against oxytocin signaling ($IC_{50} = 0.65$ μM; *SI Appendix*, Fig. S6) (54, 55). To examine whether atosiban prevents binding of inotocin to inotocin receptor, as is the case with oxytocin (56), we performed a time-resolved fluorescence resonance energy transfer (TR-FRET) assay to measure the binding efficiency between inotocin and inotocin receptor. Atosiban treatment resulted in a dose-dependent decrease in the FRET ratio ($IC_{50} = 58.8$ μM; Fig. 5*C*), indicating that it directly inhibits binding between inotocin and its receptor, thereby functioning as an antagonist of inotocin signaling. Because the inhibition effect of atosiban against inotocin signaling was not as strong as against oxytocin signaling, we performed a high-throughput chemical screening to identify novel chemical compounds acting as antagonists to inotocin signaling.

In the first screening with the 224,400 chemical compounds library, we obtained 902 compounds whose inhibition rate against inotocin signaling was >50% (Fig. 5*D*). The Z′ value (a parameter assessing the robustness of an assay for high-throughput screening) was >0.5 in all assay plates, indicating that the system was adequately optimized for the screening (Fig. 5*E*). Here, it is expected that these candidate chemicals contain nonspecific compounds blocking not only inotocin signaling but also other signaling pathways—for example, by targeting factors common with the G-protein–coupled receptor pathway. To exclude such nonspecific inhibition, we performed a second screening in which we examined the inhibitory effects of each compound against both inotocin and oxytocin signaling (Fig. 5*F*). If the effector site of these candidates is the inotocin receptor itself, the inhibition rate against oxytocin signaling should be weaker than against inotocin signaling. Twenty-three compounds showed a higher inhibition rate against inotocin signaling than oxytocin signaling (pink-shaded region in Fig. 5*F*). Among these 23 candidates, 3 chemicals (named

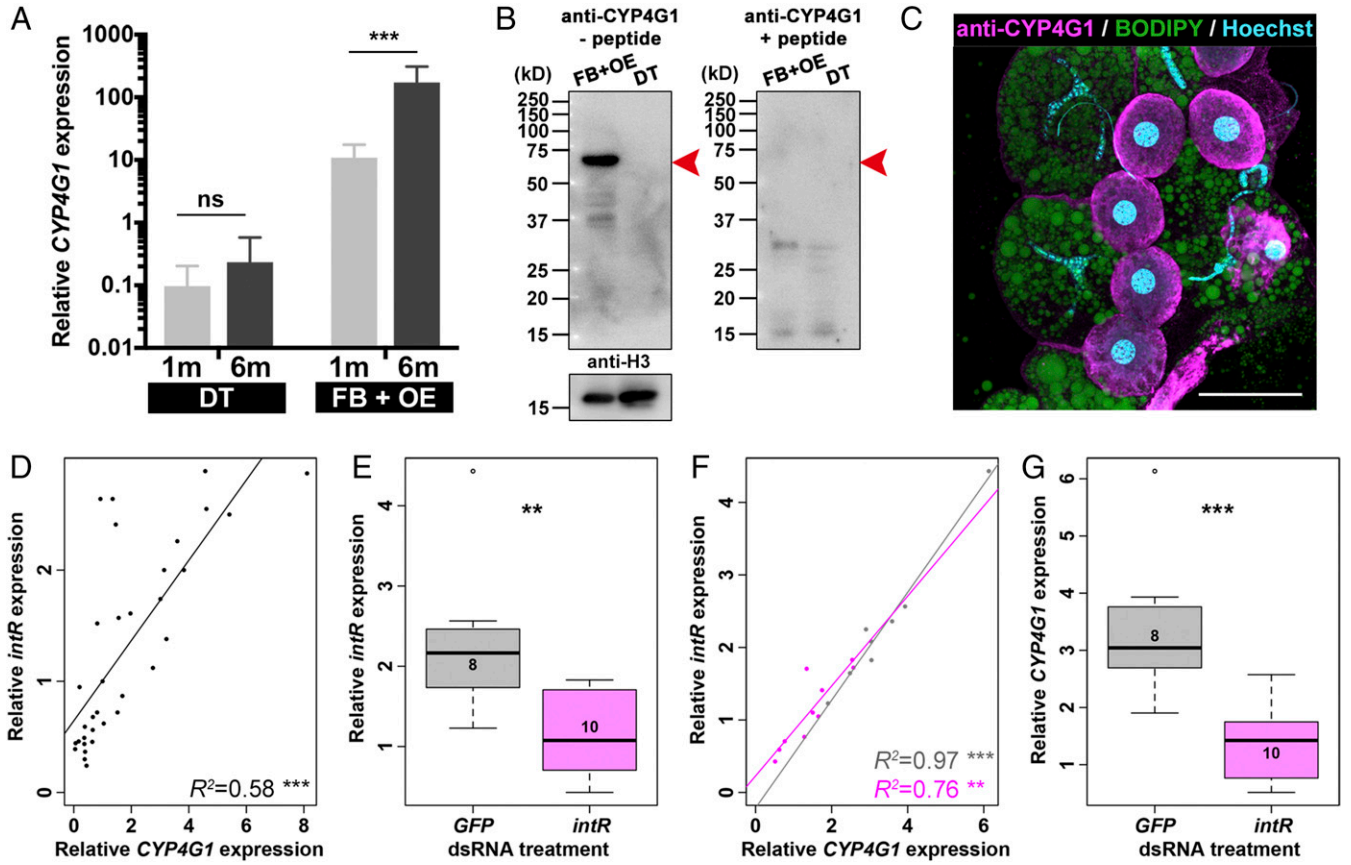

Fig. 4. Expression of CYP4G1 correlating with that of *intR*. (*A*) qRT-PCR data for *CYP4G1* expression in the digestive tract (DT) and fat body plus oenocytes (FB+OE) for 1- and 6-mo-old individuals. ns, $P > 0.05$; ***$P < 0.001$ (GLMM with Benjamini–Hochberg post hoc tests). (*B*) The CYP4G1 protein is expressed in the fat body plus oenocytes (FB+OE), but not in the digestive tract (DT). The band at 63 kDa (shown with red arrowhead in *B*, *Left*) was not detected with the anti-CYP4G1 antibody after the absorption with its antigen peptide (*B*, *Right*). (*C*) The CYP4G1 protein (magenta) is specifically present in the oenocytes (round-shaped nucleus stained with Hoechst; light blue), but not in the trophocytes (irregular-shaped nucleus and lipid droplets labeled with BODIPY; green). (Scale bar, 50 μm.) (*D*) Correlation between the expression of *CYP4G1* and *intR* in the abdomen. R^2 and *P* values are shown on the lower right of the graph. ***$P < 0.001$. (*E*) Feeding of dsRNA targeting *intR* leads to a significant decrease in the level of expression of *intR* (magenta; unpaired two-tailed *t* test, **$P < 0.01$) compared with feeding of dsRNA targeting *GFP* (gray). Number of individuals is shown in each box. (*F*) Relationship between the expression levels of *intR* and *CYP4G1* in the treatment with dsRNA targeting *GFP* (gray) and *intR* (magenta). R^2 and *P* values for each treatment are shown on the lower right of the graph. **$P < 0.01$; ***$P < 0.001$. (*G*) *CYP4G1* expression is significantly down-regulated with feeding dsRNA targeting *intR* (magenta; unpaired two-tailed *t* test) compared with feeding of dsRNA targeting *GFP* (gray). Number of individuals is shown in each box.

compounds A, B, or C in Fig. 5*G*) showed an inhibition rate that was less than half on oxytocin signaling than on inotocin signaling, even in tests with the higher dosage (20 μM) of each compound. These three chemicals also showed a dose-dependent inhibition against inotocin signaling (Fig. 5*H*) and were therefore selected for studying the role of inotocin signaling on CHC synthesis.

Regulation of CHC Synthesis via Inotocin Signaling. To study the effect of antagonists in vivo, we injected compounds A, B, and C into 4-mo-old workers and examined the expression of *CYP4G1* with quantitative RT-PCR (qRT-PCR). If these compounds inhibit inotocin signaling, the injection of each compound should, similar to the *intR* dsRNA treatment, lead to a down-regulation of *CYP4G1* expression. Consistent with this reasoning, *CYP4G1* expression was lower in workers injected with compounds A, B, and C, although the difference was only significant for compound B ($P = 0.042$; Fig. 6*A*). In addition, we found that *CYP4G1* expression was also significantly down-regulated by atosiban (1 mM, $P = 0.026$; 2 mM, $P = 0.0002$; *SI Appendix*, Fig. S7*A*). These results, together with those of the dsRNA treatment, indicate that inotocin signaling positively regulates *CYP4G1* expression.

We next examined whether down-regulation of *CYP4G1* expression has a quantitative effect on the expression of CHCs by testing compound B, the antagonist that most effectively inhibited inotocin signaling in vitro (Fig. 5*H*) and significantly down-regulated the expression of *CYP4G1* (Fig. 6*A*). In *C. fellah*, and broadly speaking in ants, CHCs are mostly composed of long-chain saturated (normal) and methyl-branched (branched) alkanes (37). We found that the quantity of normal alkanes was higher in foragers than nurses ($F_{22} = 9.4$, $P = 0.006$; *SI Appendix*, Fig. S8*A*), although neither the quantities of branched alkanes ($F_{22} = 1.1$, $P = 0.3$; *SI Appendix*, Fig. S8*B*) nor total alkanes ($F_{22} = 0.6$, $P = 0.45$; *SI Appendix*, Fig. S8*C*) was significantly different between the two types of workers. By comparing the quantity of CHCs between control and compound-B-injected >5-mo-old workers, we found that compound-B-treated ants had reduced quantities of normal alkanes ($F_{28} = 13.5$, $P = 0.001$; Fig. 6*B*) and branched alkanes ($F_{27} = 16.5$, $P = 0.0004$; Fig. 6*C*). Accordingly, the total quantity of alkanes was also significantly lower ($F_{27} = 16.7$, $P = 0.0004$; Fig. 6*D*). Injection of 2 mM atosiban also led to reduced quantities of normal alkanes ($F_{40} = 7.75$, $P = 0.008$; *SI Appendix*, Fig. S7*B*) and a tendency for reduced branched alkanes ($F_{40} = 3.1$, $P = 0.088$; *SI Appendix*, Fig. S7*C*),

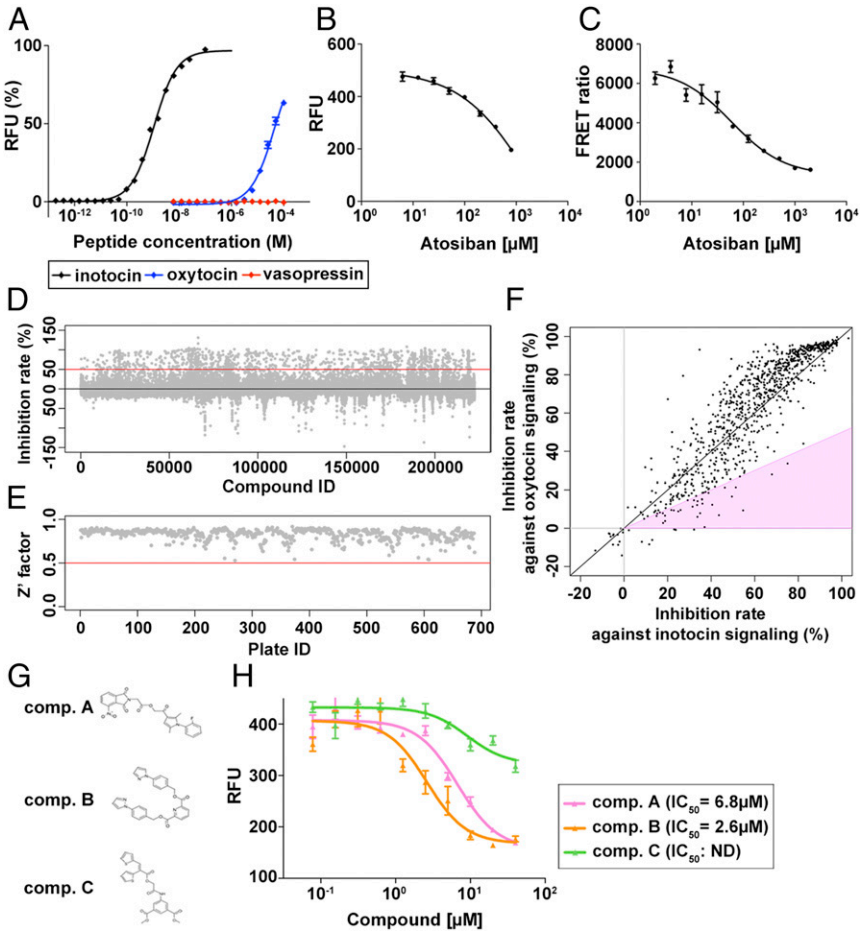

Fig. 5. Chemical screening to identify the inhibitor against inotocin signaling. (*A*) Relative fluorescence units (RFU) of Fluo-4 probe in response to inotocin, oxytocin, and vasopressin in CHO cells expressing inotocin receptor. Inotocin receptor is activated by inotocin (black line; EC_{50} = 1.1 nM) and oxytocin (blue line; EC_{50} = 41.6 μM), but not by vasopressin (red line). (*B*) Atosiban blocks the activation of inotocin signaling (IC_{50} = 599 μM). A concentration of 5 nM inotocin was used as an approximate EC_{80} concentration. Data represent the mean ± SEM (n = 3). (*C*) Competition curve of specific binding of 10 nM labeled inotocin ligand with increasing concentrations of atosiban (1.95 μM to 2 mM) measured by TR-FRET. Data represent the mean ± SEM of a representative experiment (n = 3). TR-FRET ratio = (665-nm acceptor signal/620-nm donor signal) × 10,000. (*D*) Scatter plot showing the inhibition rate of each compound in the first screening. The red line indicates a 50% inhibition. (*E*) Scatter plot showing the Z′ factor for each plate in the first screening. All Z′ factors in each plate are >0.5 indicated by the red line. (*F*) Inhibition rate against inotocin and oxytocin signaling are plotted for each of the 902 compounds showing >50% inhibition rate in the first screening. Compounds showing <0.5 ratio for oxytocin inhibition rate versus inotocin inhibition rate are in the pink-shaded region. (*G*) Structure of three compounds, A, B, and C. (*H*) Dose-dependent inhibition against inotocin signaling of compound (comp.) A (IC_{50} = 6.8 μM; pink line), comp. B (IC_{50} = 2.6 μM; orange line), and comp. C (IC_{50}; no data; green line). Data represent the mean ± SEM of a representative experiment (n = 4). RFU indicates the activation of inotocin receptor calculated from Fluo-4 intensity.

with the effect that the total quantity of alkanes was also significantly lower (F_{40} = 6.87, P = 0.012; *SI Appendix*, Fig. S7*D*).

If down-regulation of *CYP4G1* decreases production of CHCs, we predicted that ants treated with compound B should have lower resistance to desiccation and survive less well in an environment where water intake is restricted. To test this, we compared the survivability of workers fed with 1 μM compound B (treatment) with those treated with 1% DMSO (control) when given no access to water. We first confirmed that ants fed with compound B had a tendency for lower expression of *CYP4G1* than control ants (F_{22} = 4.03, P = 0.057; Fig. 6*E*), as previously observed in the injection assays (Fig. 6*A*). To manipulate desiccation rates, we placed seven workers in a box at either 55% relative humidity (RH) or 85% RH. Under 55% RH, both treatment and control workers died rapidly, and there was no difference in survival (P = 0.76), suggesting that these experimental conditions were too severe for ants, regardless of treatment. Under the 85% RH condition, both treatment and control groups survived significantly longer (P < 0.0001; Fig. 6*F*), and there was a significant lower survival for ants treated with compound B compared with control ants (P = 0.026; Fig. 6*F*). This suggests that in conditions where water is absent, ants are capable of surviving longer with intact *CYP4G1* and CHC function.

Discussion

Our study reveals that the levels of *int* and *intR* mRNA are very high in workers and positively correlated with age and foraging behavior. Moreover, when ants of the same age were placed into a new artificial nest and allowed to reestablish division of labor, those initiating foraging had higher levels of *int* or *intR* expression than those staying within the nest, suggesting that inotocin signaling may be linked to the onset of foraging behavior in ants. The levels of expression of oxytocin and vasopressin is known to also influence social behavior in mammals. For example, the level of social investigation is associated with the level of expression of *oxytocin* and *vasopressin* mRNA in mice (57). In mice, the level of expression of *vasopressin* is also correlated with aggressive behavior (58, 59), while oxytocin signaling is involved with social bonding and affiliation (4, 60, 61).

CHCs are known to prevent desiccation in insects (33–35), and recent work on flies supports the hypothesis that increased CHC production improves desiccation resistance (62). In ants, dessication is an important challenge when workers switch tasks and initiate foraging. We found that *C. fellah* workers switch tasks when they are 4 mo old. Similar results were obtained in other studies (32, 47). As workers age, they experience a drastic change in their environment as they switch from brood care and other within-nest tasks to foraging outside of the colony. Factors such as humidity and temperature can vary greatly over time and space outside the nest, while they are relatively stable within the nest. Similar to findings in the ants *Pogonomyrmex barbatus* and *Formica exsecta* (40–43), we found task-associated variation in CHCs, with foragers exhibiting the highest proportion of normal alkanes. Moreover, experimental increments of temperature and decreases in humidity also triggered an increase in the proportion of normal alkanes in harvester ants (41). Given that we found that *intR* is expressed in the oenocytes, we investigated the relationship between inotocin signaling and the CHC-synthesis pathway. We focused on the *CYP4G1* gene, which is known to be

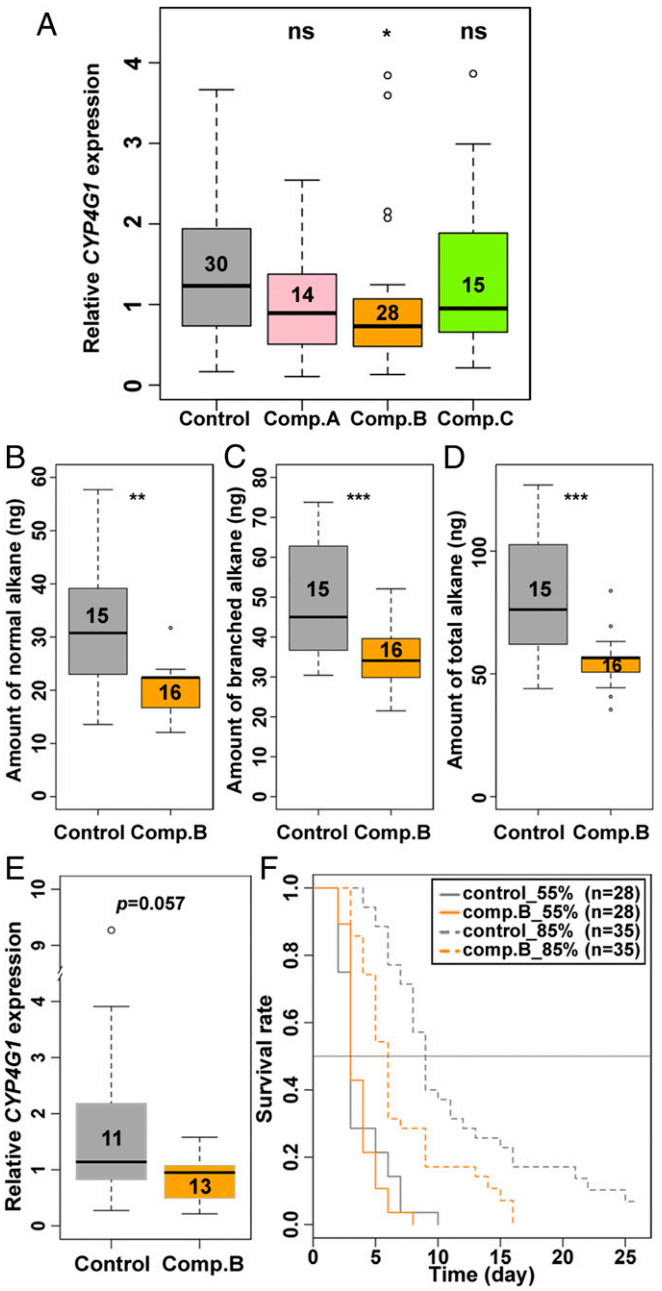

Fig. 6. Relationship between inotocin signaling, hydrocarbon synthesis, and desiccation resistance. (*A*) *CYP4G1* expression (qRT-PCR) for comp. A-, B-, and C-treated and control 4-mo-old workers. ns, $P > 0.05$; $*P < 0.05$ (GLMM with Dunnett post hoc tests). (*B–D*) The quantities of normal (*B*), branched (*C*), and total alkanes (*D*) in comp. B-treated and control >5-mo-old workers. $**P < 0.01$; $***P < 0.001$. (*E*) qRT-PCR for *CYP4G1* in comp. B-fed and control 4-mo-old workers. Number of individuals is shown in each box. The data were analyzed with GLMMs. (*F*) Survival curves for control (gray) and comp. B-treated (orange) ants in 55% RH (solid line) or 85% RH (dashed line). Sample sizes are as follows; $n = 28$ for ctrl_55% and comp. B_55%, and $n = 35$ for ctrl_85% and comp. B_85%.

expressed in oenocytes (44–46), where it regulates the final step of CHC synthesis by converting aldehyde to hydrocarbons (45). Using immunohistochemistry, we first confirmed that the CYP4G1 protein is specifically expressed in the oenocytes in workers. Next, we showed a strong positive association between the levels of expression of *intR* and *CYP4G1*, suggesting that increased levels of *intR* expression might be associated with increased levels of *CYP4G1* when workers start foraging. These lines of evidence suggest that foraging ants are able to reduce the risk of desiccation through up-regulation of the inotocin signaling pathway, generating elevated quantities of protective CHCs.

Because variation in task allocation is associated with variation in CHCs not only in *C. fellah* (this study), but also in the two other ants that have been investigated so far (i.e., *P. barbatus* and *F. exsecta*; refs. 40–43), it would be interesting to test whether inotocin signaling does also regulate the production of CHCs in these species. In the ants *Lasius niger* and *L. neglectus*, the level of expression of *intR* has also been shown to be higher in the abdomen than in the head and thorax (21), suggesting that this gene might also be implicated in the production of CHCs. Moreover, as in *C. fellah,* the expression of *int* is also higher in the head of foragers than nurses in the ant *Monomorium pharanonis* (63). The similarity in the expression profiles of *int* and *intR* in the ant species that have been studied so far suggests that inotocin signaling may, as in *C. fellah*, also function to regulate the expression of CHCs in other ant species.

To provide functional evidence for a role of *intR* on the level of expression of *CYP4G1*, we fed 5-mo-old workers with dsRNA targeting *intR.* These treated workers exhibited a lower level of expression of both *intR* and *CYP4G1* compared with control ants. Next, we conducted pharmacological studies to identify compounds acting as antagonists of the inotocin-signaling pathway. These studies identified three effective antagonist compounds (named A, B, and C). Injection of these antagonists led to decreased expression of *CYP4G1.* Finally, *CYP4G1* expression was also significantly down-regulated by atosiban, an inhibitor of oxytocin in vertebrates (64, 65), which we showed to also be effective in decreasing the activation of inotocin receptor by inotocin in vitro. Together, these results show that inotocin signaling positively regulates *CYP4G1* expression.

Our experiments also showed that workers treated with compound B had reduced quantities of normal and branched alkanes and a lower survival than control workers under water-limited conditions. These findings are interesting because *int* and its receptor are both up-regulated when workers age and switch tasks from nursing to foraging. Since workers are more likely to encounter drier environments when they forage, this suggests that inotocin signaling may be implicated in regulating physiological adaptations via increased CHC synthesis when workers initiate foraging.

Our study provides evidence that the inotocin-signaling pathway regulates CHC synthesis via *CYP4G1* expression in insects, and this pathway is up-regulated with age and task preference in ants. Interestingly, genomic studies revealed that the inotocin-signaling pathway has been lost in the honey bee and some other species of aphids and flies (16). As these species have the *CYP4G* gene (45) and express CHCs on their body surface, it is possible that other signaling pathways have taken over the functions of inotocin signaling in these species, as discussed (16, 22). It will therefore be of interest to compare the mechanisms of regulation of *CYP4G* gene and CHCs in these species that have lost the inotocin-signaling pathway. Such comparative studies may also shed light on the ancestral role of the oxytocin/vasopressin family peptide in insects and vertebrates.

Methods

More details are provided in *SI Appendix*.

Ants. *C. fellah* colonies were initiated from queens collected after a mating flight in March 2003 and 2007 in Tel Aviv. The ants were reared in an incubator (Nippon Medical & Chemical Instruments Co., Ltd.) under controlled conditions [12:12 light:dark (LD), 30 °C, 55~60% RH]. For all experiments, we used workers from four queenright colonies that each had 1 queen and ~500 workers. We used only minor workers with a body size <8 mm. To determine their age, we painted every month all newly eclosed workers with a unique color code. Young virgin queens, males, and workers were collected at the beginning of mating flights in May 2015 and 2016 in Tokyo and Ibaraki, Japan

(*C. japonicus*) and March in 2018 in Rehovot, Israel (*C. fellah*). Wingless mated queens of both species were collected on the ground just after the mating flight.

qRT-PCR. RNA was extracted with TRIzol (Invitrogen) from whole body (Fig. 2 *F–K*), body parts (Figs. 1, 2 *C* and *D*, 4 *D–G*, and 6 *A* and *E* and *SI Appendix*, Figs. S1, S5, and S7*A*), or dissected tissues (Figs. 3*L* and 4*A*). RNA from queens was sequentially purified with the RNA Plus Micro Kit (Qiagen). cDNA was synthesized from 200 ng of total RNA by using a PrimeScript RT Reagent Kit with gDNA Eraser (Takara). qRT-PCR was performed with Takara SYBR Premix Ex Taq II (Tli RNaseH Plus) by using 7900HT (Applied Biosystems), a LightCycler 480 (Roche), or MX3000P (Agilent). Primers for qRT-PCR are listed in *SI Appendix*, Table S2. All primers had similar PCR amplification efficiency (~2.0). The most stable reference genes and gene-normalization factors were determined by the software geNORM with Biogazelle software (qbase). We used *ef1a* and *rp2* for whole-body, head, and abdomen analyses and *gapdh* and *rp2* for the fat body plus oenocyte and digestive-tract analyses. The relative expressions of target genes were scaled against average values in each experiment with the Biogazelle software (qbase).

Quantification of Peptide with LC-MS/MS. The detailed procedure for peptide extraction is shown in *SI Appendix*. The amount of inotocin peptide was quantified by ultraperformance LC (ACQUITY System, Waters), equipped with a tandem mass spectrometer, TQD (Waters). Separation was achieved on an AccQ-Tag Ultra RP Column (2.1 × 100 mm, 1.7-μm particles; Waters) at 40 °C. The two mobile phases consisted of (*i*) 20 mM formic acid and (*ii*) acetonitrile. Linear gradients from 99.9% (*i*) to 50% (*i*) were used for the separation at a flow rate of 0.3 mL/min. The effluent was then introduced into TQD, ionized by electrospray ionization with positive ion mode, and detected by multiple-reaction monitoring using the transition of *m/z* 328.4 to 86.38. Sample concentrations were calculated from the standard curve obtained from serial dilution of synthesized inotocin peptide (Biogate Co., Ltd).

DNA Constructs. The cDNA of the *int* and *intR* was obtained by reverse transcription using the Prime script RT Reagent Kit with gDNA eraser (Takara) and RNA isolated from whole body of *C. fellah* and *C. japonicus* worker from the laboratory colony. The oxytocin receptor (OXTR) and Gα15 were amplified from the following vectors, respectively: human OXTR in pcDNA3.1+ (cDNA Resource Center, catalog no. OXTR00000) and human Gα15 in pcDNA3.1+ (cDNA Resource Center catalog no. GNA1500000). Detailed procedures to construct *pPB-intR-* and *pPB-OXTR-mcherry* are shown in *SI Appendix*.

Generation of Antibodies. Polyclonal rabbit antibody to inotocin proprotein was generated with a synthetic peptide CKISDVADREITDLYMVLSGNEVSNEILP, corresponding to the C terminus of inotocin proprotein (MBL Co., Ltd.). Polyclonal rabbit antibody to CYP4G1 was generated with a synthetic peptide, RDDLDDIDENDRGEKRRLA, corresponding from 301- to 319-aa sequence of CYP4G1 (Hokudo Co., Ltd.). The antibodies were used for immunostaining (Figs. 3 *D–J* and 4*C* and *SI Appendix*, Fig. S4*D*) and Western blot (Fig. 4*B* and *SI Appendix*, Fig. S4 *B* and *C*).

Western Blot Analysis. We subjected tissue lysates to 12.5% SDS/PAGE analysis and immunoblotting. Rabbit polyclonal antibody to inotocin (1:50), rabbit polyclonal antibody to CYP4G1 (1:500), anti-Histone H3 antibody (1:500; Cell Signaling), anti-myc (1:1,000; Invitrogen), anti–β-tubulin (1:2,000; Invitrogen), and anti-gapdh (1:2,000; Cell Signaling) were used as primary antibodies, whereas horseradish peroxidase-conjugated antibody to rabbit (1:1,000; Cell Signaling) and antibody to mouse (1:1,000; Promega) were used as secondary antibodies. Immobilon Western (Millipore) was used for detection. As negative control, we mixed in a ratio of 1:20 (mol) the antibodies for inotocin and CYP4G1 with their synthesized antigen peptides incubated at 4 °C overnight. After the overnight incubation, they were stored in 50% glycerol at −20 °C. Images were captured with the LAS4000 (GE Healthcare ImageQuant) or Chemidoc XRS+ systems (Bio-Rad).

Immunohistochemistry. Whole-brain immunohistochemistry was performed as described (66) with some modifications in *SI Appendix*. Fluorescent images were captured with TCS-SP5 laser-scanning confocal microscopy (Leica) with a HC PL Fluotar 10×/0.30 objective (catalog no. 506505, Leica) or HC PL APO 20×/0.70 objective (catalog no. 506513, Leica) and the Application Suite Advanced Fluorescence software (Leica) or LSM700 laser-scanning confocal microscopy (Carl Zeiss) with a Plan-APOCHROMAT 10×/0.45 or 20×/0.8 objective (Carl Zeiss) and ZEN 2011 software.

In Situ Hybridization. To examine *int* mRNA expression in the brain, fluorescence in situ hybridization was performed by using the RNAscope Multiplex Fluorescent Reagent Kit 2.0, according to the manufacturer's instructions (Advanced Cell Diagnostics). Detailed protocol is shown in *SI Appendix*.

dsRNA Generation and Treatment. Gene-specific 520-bp sequences for *intR* (1–520 bp) and control *EGFP* (104–623 bp) with T7 RNA polymerase sequence at both ends were amplified by PCR with primers listed in *SI Appendix*, Table S3, and in vitro transcription was performed by using the T7 RiboMAX Express RNAi System (Promega), according to the manufacturer's protocol. The concentration and the size of dsRNA were determined with a nanodrop spectrophotometer and electrophoresis. dsRNA was adjusted to 4 μg/μL with 300 mM sucrose water. The feeding treatments with dsRNA were performed as described (51). For first 10 d of the treatment, ants were fed daily with 20 μL of dsRNA–sucrose water and then with 20 μL of sucrose water with no dsRNA during the last 5 d. After these 15-d treatments, RNA was extracted from each body part for qRT-PCR analyses.

Calcium Assay and Chemical Screening. The protocol to generate stable cell lines and cell preparation for calcium assay is shown in *SI Appendix*. We used the Functional Drug Screening System (FDSS7000; Hamamatsu Photonics) to measure the fluorescence level of Fluo-4 with the excitation and emission wavelength bands centered at 480 and 540 nm, respectively. The ligand was diluted with the buffer (20 mM Hepes in HBSS) and dispensed to the nonbinding 384-well plate (Greiner). A total of 5 μL of ligand solution was dispensed to each well with a plastic tip (Hamamatsu Photonics) 10 s after the measurement started. The fluorescent intensity was measured for 2 min in each plate. The ligands were washed away between each experiment with a cleaning solution [10 mM citric acid (Nakarai) in 50% ethanol]. The fluorescence intensity from 1 to 10 s or from 11 to 120 s in the measurement was used in the following formula. Response to the ligand (R) was given by

$$R = \mathrm{Max}\,(\mathrm{Intensity}_{11-120}) - \mathrm{Average}(\mathrm{Intensity}_{1-10}).$$

We performed the chemical screening with 222,400 compounds obtained from the Drug Discovery Initiative (The University of Tokyo). Detailed procedures for first and second chemical screening are shown in *SI Appendix*.

Binding Assay with TR-FRET. Inotocin receptor ligand-binding assays were performed by using the Tag-lite assay (cisbio), according to the manufacturer's instructions shown in *SI Appendix*.

Antagonist Injection. To select the appropriate dosage of each compound for injection, we first examined the effect of DMSO on ant survivability, because compounds A, B, and C were stocked in DMSO (10 mM concentration). We found that 1% DMSO showed no effect on survivability, while 10% DMSO resulted in high lethality. Therefore, we injected 100 μM compound A (catalog no. PB03670558; U.O.S.), B (catalog no. PB153374836; U.O.S.), or C (catalog no. T5275621; Enamine) in 1% DMSO to avoid negative effects of DMSO. Because atosiban (Sigma-Aldrich) had a weaker inhibition rate (Fig. 5*B*) than compound A, B, or C (Fig. 5*H*) in vitro and because it is soluble in water, we used higher concentrations (1 and 2 mM). Ants were anesthetized on ice and injected into the abdomen through the intersegmental membrane with 1.5 μL of the different compound solution with an IM-300 microinjector (Narishige). Control saline was prepared as the mixture of ant saline with the solvent of each chemical compounds [with water for atosiban (1:10 for 1 mM and 1:5 for 2 mM) and with DMSO for compounds A, B, and C (1:100)]. For the expression analysis of *CYP4G1*, RNA was extracted at 24 h after the injection of each compound.

Behavior Tracking System and Tracking Data Processing. Behavioral tracking was performed as described (47). Ants were tagged with unique matrix codes (1.6-mm side length) after immobilization on ice. Tracking experiments were performed under controlled conditions (12:12 LD, 30 °C, 55~60% RH). The tracking data were postprocessed as described (47). Parameters for time spent in the food, distance ant moved, and time spent in the nest were obtained as described (67).

CHC Analysis. The extraction and quantification of CHCs was performed as described (68) with some modifications. Detailed protocol is shown in *SI Appendix*.

ACKNOWLEDGMENTS. We thank A. Hefetz and O. Feinerman for collecting queens; Y. Yamaguchi and T. Chihara for supplying plasmids; A. Crespi and D. Mersch for the technical support for the tracking system; C. Stoffel and C. La Mendola for gene-expression analyses; M. Sakurai, Y. Mawatari, and A. Nakamichi for help with animal-keeping, gene expression, and immunohistochemistry analyses; H. Watanabe for technical support for

the study of neural anatomy; M. Hojo and M. Kanno for help with analyses of CHCs; F. Obata for support in peptide quantification; A. LeBoeuf, T. Onaka, T. Kikusui, R. Benton, and T. Tamura for helpful discussions; and T. Fukatsu and members of the Symbiotic Evolution and Biological Functions Research Group for the technical assistance and advice. This work was supported by Japan Society for the Promotion of Science Grant-in-Aid for Scientific Research on Innovative Areas 4501; Japan Agency for Medical Research and Development (AMED) Grant JP18gm6110014; and in part by AMED Platform Project for Supporting Drug Discovery and Life Science Research Grant JP17am0101086 and the Swiss National Science Foundation. The funders had no role in the study design, data collection and analysis, decision to publish, or preparation of the manuscript.

1. Feldman R, Weller A, Zagoory-Sharon O, Levine A (2007) Evidence for a neuroendocrinological foundation of human affiliation: Plasma oxytocin levels across pregnancy and the postpartum period predict mother-infant bonding. *Psychol Sci* 18:965–970.
2. Kosfeld M, Heinrichs M, Zak PJ, Fischbacher U, Fehr E (2005) Oxytocin increases trust in humans. *Nature* 435:673–676.
3. Parreiras-E-Silva LT, et al. (2017) Functional New World monkey oxytocin forms elicit an altered signaling profile and promotes parental care in rats. *Proc Natl Acad Sci USA* 114:9044–9049.
4. Ross HE, Young LJ (2009) Oxytocin and the neural mechanisms regulating social cognition and affiliative behavior. *Front Neuroendocrinol* 30:534–547.
5. Ferris CF, Axelson JF, Martin AM, Roberge LF (1989) Vasopressin immunoreactivity in the anterior hypothalamus is altered during the establishment of dominant/subordinate relationships between hamsters. *Neuroscience* 29:675–683.
6. Ferris CF, Pollock J, Albers HE, Leeman SE (1985) Inhibition of flank-marking behavior in golden hamsters by microinjection of a vasopressin antagonist into the hypothalamus. *Neurosci Lett* 55:239–243.
7. Terranova JI, Ferris CF, Albers HE (2017) Sex differences in the regulation of offensive aggression and dominance by arginine-vasopressin. *Front Endocrinol (Lausanne)* 8:308.
8. Winslow JT, Hastings N, Carter CS, Harbaugh CR, Insel TR (1993) A role for central vasopressin in pair bonding in monogamous prairie voles. *Nature* 365:545–548.
9. Martos-Sitcha JA, Campinho MA, Mancera JM, Martínez-Rodríguez G, Fuentes J (2015) Vasotocin and isotocin regulate aquaporin 1 function in the sea bream. *J Exp Biol* 218:684–693.
10. Hasegawa T, Tanii H, Suzuki M, Tanaka S (2003) Regulation of water absorption in the frog skins by two vasotocin-dependent water-channel aquaporins, AQP-h2 and AQP-h3. *Endocrinology* 144:4087–4096.
11. Goodson JL, Schrock SE, Klatt JD, Kabelik D, Kingsbury MA (2009) Mesotocin and nonapeptide receptors promote estrildid flocking behavior. *Science* 325:862–866.
12. Klatt JD, Goodson JL (2013) Oxytocin-like receptors mediate pair bonding in a socially monogamous songbird. *Proc Biol Sci* 280:20122396.
13. Oldfield RG, Hofmann HA (2011) Neuropeptide regulation of social behavior in a monogamous cichlid fish. *Physiol Behav* 102:296–303.
14. Pedersen A, Tomaszycki ML (2012) Oxytocin antagonist treatments alter the formation of pair relationships in zebra finches of both sexes. *Horm Behav* 62:113–119.
15. Yokoi S, et al. (2015) An essential role of the arginine vasotocin system in mate-guarding behaviors in triadic relationships of medaka fish (*Oryzias latipes*). *PLoS Genet* 11:e1005009.
16. Liutkeviciute Z, Koehbach J, Eder T, Gil-Mansilla E, Gruber CW (2016) Global map of oxytocin/vasopressin-like neuropeptide signalling in insects. *Sci Rep* 6:39177.
17. Douzery EJ, Snell EA, Bapteste E, Delsuc F, Philippe H (2004) The timing of eukaryotic evolution: Does a relaxed molecular clock reconcile proteins and fossils? *Proc Natl Acad Sci USA* 101:15386–15391.
18. Aikins MJ, et al. (2008) Vasopressin-like peptide and its receptor function in an indirect diuretic signaling pathway in the red flour beetle. *Insect Biochem Mol Biol* 38: 740–748.
19. Chérasse S, Aron S (2017) Measuring inotocin receptor gene expression in chronological order in ant queens. *Horm Behav* 96:116–121.
20. Gruber CW, Muttenthaler M (2012) Discovery of defense- and neuropeptides in social ants by genome-mining. *PLoS One* 7:e32559.
21. Liutkevičiūtė Z, et al. (2018) Oxytocin-like signaling in ants influences metabolic gene expression and locomotor activity. *FASEB J*, 10.1096/fj.201800443.
22. Stafflinger E, et al. (2008) Cloning and identification of an oxytocin/vasopressin-like receptor and its ligand from insects. *Proc Natl Acad Sci USA* 105:3262–3267.
23. Donaldson ZR, Young LJ (2008) Oxytocin, vasopressin, and the neurogenetics of sociality. *Science* 322:900–904.
24. Insel TR (2010) The challenge of translation in social neuroscience: A review of oxytocin, vasopressin, and affiliative behavior. *Neuron* 65:768–779.
25. Neumann ID, Landgraf R (2012) Balance of brain oxytocin and vasopressin: Implications for anxiety, depression, and social behaviors. *Trends Neurosci* 35:649–659.
26. Wilson E, Hölldobler B (1990) *The Ants* (Springer, Berlin).
27. Smith CR, Toth AL, Suarez AV, Robinson GE (2008) Genetic and genomic analyses of the division of labour in insect societies. *Nat Rev Genet* 9:735–748.
28. Robinson EJ, Feinerman O, Franks NR (2009) Flexible task allocation and the organization of work in ants. *Proc Biol Sci* 276:4373–4380.
29. Bourke AFG, Franks NR (1995) *Social Evolution in Ants* (Princeton Univ Press, Princeton).
30. Huang ZY, Robinson GE (1992) Honeybee colony integration: Worker-worker interactions mediate hormonally regulated plasticity in division of labor. *Proc Natl Acad Sci USA* 89:11726–11729.
31. Robinson GE, Page RE, Jr, Strambi C, Strambi A (1989) Hormonal and genetic control of behavioral integration in honey bee colonies. *Science* 246:109–112.
32. Seid MA, Traniello JFA (2006) Age-related repertoire expansion and division of labor in *Pheidole dentata* (hymenoptera: Formicidae): A new perspective on temporal polyethism and behavioral plasticity in ants. *Behav Ecol Sociobiol* 60:631–644.
33. Gibbs AG, Chippindale AK, Rose MR (1997) Physiological mechanisms of evolved desiccation resistance in *Drosophila melanogaster*. *J Exp Biol* 200:1821–1832.
34. Gibbs AG (1998) Water-proofing properties of cuticular lipids. *Am Zool* 38:471–482.
35. Wigglesworth V (1945) Transportation through the cuticle of insects. *J Exp Biol Lond* 21:97–114.
36. Chung H, Carroll SB (2015) Wax, sex and the origin of species: Dual roles of insect cuticular hydrocarbons in adaptation and mating. *BioEssays* 37:822–830.
37. Boulay R, Hefetz A, Soroker V, Lenoir A (2000) *Camponotus fellah* colony integration: Worker individuality necessitates frequent hydrocarbon exchanges. *Anim Behav* 59:1127–1133.
38. Ozaki M, et al. (2005) Ant nestmate and non-nestmate discrimination by a chemosensory sensillum. *Science* 309:311–314.
39. VanderMeer RK, Breed MD, Espelie KE, Winston ML (1998) *Pheromone Communication in Social Insects* (Westview Press, Boulder, CO).
40. Wagner D, et al. (1998) Task-related differences in the cuticular hydrocarbon composition of harvester ants, *Pogonomyrmex barbatus*. *J Chem Ecol* 24:2021–2037.
41. Wagner D, Tissot M, Gordon D (2001) Task-related environment alters the cuticular hydrocarbon composition of harvester ants. *J Chem Ecol* 27:1805–1819.
42. Martin SJ, Drijfhout FP (2009) Nestmate and task cues are influenced and encoded differently within ant cuticular hydrocarbon profiles. *J Chem Ecol* 35:368–374.
43. Sturgis SJ, Greene MJ, Gordon DM (2011) Hydrocarbons on harvester ant (*Pogonomyrmex barbatus*) middens guide foragers to the nest. *J Chem Ecol* 37:514–524.
44. Fan Y, Zurek L, Dykstra MJ, Schal C (2003) Hydrocarbon synthesis by enzymatically dissociated oenocytes of the abdominal integument of the German cockroach, *Blattella germanica*. *Naturwissenschaften* 90:121–126.
45. Qiu Y, et al. (2012) An insect-specific P450 oxidative decarbonylase for cuticular hydrocarbon biosynthesis. *Proc Natl Acad Sci USA* 109:14858–14863.
46. Yu Z, et al. (2016) *LmCYP4G102*: An oenocyte-specific cytochrome P450 gene required for cuticular waterproofing in the migratory locust, *Locusta migratoria*. *Sci Rep* 6:29980.
47. Mersch DP, Crespi A, Keller L (2013) Tracking individuals shows spatial fidelity is a key regulator of ant social organization. *Science* 340:1090–1093.
48. Bloch G, Solomon SM, Robinson GE, Fahrbach SE (2003) Patterns of PERIOD and pigment-dispersing hormone immunoreactivity in the brain of the European honeybee (*Apis mellifera*): Age- and time-related plasticity. *J Comp Neurol* 464:269–284.
49. Arrese EL, Soulages JL (2010) Insect fat body: Energy, metabolism, and regulation. *Annu Rev Entomol* 55:207–225.
50. Roma GC, Bueno OC, Camargo-Mathias MI (2010) Morpho-physiological analysis of the insect fat body: A review. *Micron* 41:395–401.
51. Ratzka C, Gross R, Feldhaar H (2013) Gene expression analysis of the endosymbiont-bearing midgut tissue during ontogeny of the carpenter ant *Camponotus floridanus*. *J Insect Physiol* 59:611–623.
52. Di Giglio MG, et al. (2017) Development of a human vasopressin V_{1a}-receptor antagonist from an evolutionary-related insect neuropeptide. *Sci Rep* 7:41002.
53. Simhan HN, Caritis SN (2007) Prevention of preterm delivery. *N Engl J Med* 357:477–487.
54. Herington JL, et al. (2015) High-throughput screening of myometrial calcium-mobilization to identify modulators of uterine contractility. *PLoS One* 10:e0143243.
55. Maggi M, et al. (1994) Antagonists for the human oxytocin receptor: An *in vitro* study. *J Reprod Fertil* 101:345–352.
56. Gimpl G, Postina R, Fahrenholz F, Reinheimer T (2005) Binding domains of the oxytocin receptor for the selective oxytocin receptor antagonist barusiban in comparison to the agonists oxytocin and carbetocin. *Eur J Pharmacol* 510:9–16.
57. Clipperton-Allen AE, et al. (2012) Oxytocin, vasopressin and estrogen receptor gene expression in relation to social recognition in female mice. *Physiol Behav* 105:915–924.
58. Steinman MQ, et al. (2015) Hypothalamic vasopressin systems are more sensitive to the long term effects of social defeat in males versus females. *Psychoneuroendocrinology* 51:122–134.
59. Terranova JI, et al. (2016) Serotonin and arginine-vasopressin mediate sex differences in the regulation of dominance and aggression by the social brain. *Proc Natl Acad Sci USA* 113:13233–13238.
60. Lee HJ, Macbeth AH, Pagani JH, Young WS, 3rd (2009) Oxytocin: The great facilitator of life. *Prog Neurobiol* 88:127–151.
61. Nagasawa M, et al. (2015) Social evolution. Oxytocin-gaze positive loop and the coevolution of human-dog bonds. *Science* 348:333–336.
62. Ferveur JF, Cortot J, Rihani K, Cobb M, Everaerts C (2018) Desiccation resistance: Effect of cuticular hydrocarbons and water content in *Drosophila melanogaster* adults. *PeerJ* 6:e4318.
63. Gospocic J, et al. (2017) The neuropeptide corazonin controls social behavior and caste identity in ants. *Cell* 170:748–759.e12.
64. Manning M, et al. (2012) Oxytocin and vasopressin agonists and antagonists as research tools and potential therapeutics. *J Neuroendocrinol* 24:609–628.
65. Melin P, Trojnar J, Johansson B, Vilhardt H, Akerlund M (1986) Synthetic antagonists of the myometrial response to vasopressin and oxytocin. *J Endocrinol* 111:125–131.
66. Ott SR (2008) Confocal microscopy in large insect brains: Zinc-formaldehyde fixation improves synapsin immunostaining and preservation of morphology in whole-mounts. *J Neurosci Methods* 172:220–230.
67. Koto A, Mersch D, Hollis B, Keller L (2015) Social isolation causes mortality by disrupting energy homeostasis in ants. *Behav Ecol Sociobiol* 69:583–591.
68. Hojo MK, et al. (2009) Chemical disguise as particular caste of host ants in the ant inquiline parasite *Niphanda fusca* (Lepidoptera: Lycaenidae). *Proc Biol Sci* 276: 551–558.